Physica A 561 (2021) 125266

Contents lists available at ScienceDirect

Physica A

journal homepage: www.elsevier.com/locate/physa

Dynamic model with super spreaders and lurker users for preferential information propagation analysis

Minglei Fu [a,*], Jun Feng [a], Dmytro Lande [b], Oleh Dmytrenko [b], Dmytro Manko [b], Ryhor Prakapovich [c]

[a] College of Information Engineering, Zhejiang University of Technology, Hangzhou 310023, China
[b] Institute for Information Recording, National Academy of Sciences of Ukraine, Kiev 03113, Ukraine
[c] United Institute of Informatics Problems, National Academy of Sciences of Belarus, Minsk 220012, Belarus

ARTICLE INFO

Article history:
Received 27 May 2019
Received in revised form 8 January 2020
Available online 16 September 2020

Keywords:
Complex system
Social network
Dynamic model
Threshold
Preferential information

ABSTRACT

Publication of preferential information via online social networks has recently increased in business promotional activities. This activity involves consideration of the propagation of preferential information in online social networks as well as the effects of such propagation on shopping choices. This paper proposes the susceptible-lurker-super-normal-recovered (SEAIR) dynamics model to address the propagation process of preferential information in the Weibo network. In the proposed SEAIR model, super spreader and lurker user compartments are adopted, and entry and exit are available to and from every compartment, which more realistically reflects circumstances in Weibo. Dynamic equations of the SEAIR model are proposed based on the mean-field theory, and the basic reproductive ratio (threshold) $\mathcal{R}_0$ derived. Furthermore, it is proved that the information-free equilibrium state of the SEAIR model is locally and globally stable when $\mathcal{R}_0$ is less than one, at which point the propagation process tends to disappear; there is a unique endemic equilibrium state when $\mathcal{R}_0$ is greater than one. To verify the performance of the SEAIR model, a Baidu App promotion activity in Weibo is used as a real case study. Compared to the conventional susceptible–infected–recovered (SIR) model, numerical results show that the SEAIR model reduces the root mean square error (RMSE) and the mean absolute error (MAE) by 33.2% and 24.74%, respectively. The influence of the main parameters on the performance of the SEAIR model are also analyzed.

1. Introduction

The popularity of the mobile internet has resulted in online social media being the preferred platform for sharing, disseminating, and obtaining information. Business promotional activities are increasingly being executed via online social media, including the publication of preferential information and product advertisements. Hence, research on the propagation of preferential information in online social networks and its effect on shopping choices is becoming increasingly relevant [1,2]. Propagation dynamic models of preferential information have attracted significant attention from researchers. For example, Wan et al. proposed a novel susceptible infected beneficial model based on scale-free networks [1]. They discovered that when preferential information is obtained from infected and beneficial users, users

* Corresponding author.
E-mail address: fuml@zjut.edu.cn (M. Fu).

https://doi.org/10.1016/j.physa.2020.125266
0378-4371/

could be infected users according to two different probabilities. Fu et al. developed a follower super forwarder client (FSFC) model based on the susceptible–infected–recovered (SIR) model [2], and verified its feasibility for describing the spreading behavior of preferential information in online social networks.

Similarities exist between the spreading processes of information propagation among users and that of epidemic disease among individuals [3–5]; the latter has been extensively studied since Barabási et al. discovered the scale-free nature of social networks [6]. The scale-free and small-world characteristics in real-world networks have accelerated the study of complex networks as well as the determination of information propagation characteristics of real networks based on infectious disease models in complex networks. Daley and Kendal proposed the rumor propagation DK model based on the basic infectious disease model [7]. In the DK model, individuals are divided into three parts: those unaware of the message, spreaders, and those aware of the message that do not propagate it. Additionally, some studies have found that the complexity of human behavior and the characteristics of diversity affect the process of information dissemination [8–11].

In the past five years, studies have increasingly focused on the improvement of information propagation dynamics models. Zan et al. proposed two new models as an extension of the SIR model, the SICR and the adjusted-SICR model, by considering the counterattack mechanism of rumor spreading [12]. Zhu et al. proposed the improved SEIR model as an extension of the SIR model with the addition of exposed compartments and consideration of the characteristics of the evolution of user opinions [13]. By adding hesitators as a neutralized state of dual information competition, Yun et al. developed the SHIR model based on the SIR model [14]. Wang et al. proposed the SEINR model, which focuses on the different propagation characteristics of different spreaders in network information dissemination. In the SEINR model, the spreaders in the network are divided into N categories for information dissemination simulation [15]. Zhao et al. proposed the SIHR rumor spread model by considering the characteristics of users forgetting and recalling information [16]. Zan studied the propagation characteristics of double opinion information in the network in the DSIR model [17].

According to the characteristics of network information dissemination, additional improved models have been proposed based on the basic infectious disease models [18–23]. Yu et al. analyzed the bifurcation of the SEIR model with the latent state and SIR model [24]. Hosseini et al. proposed the SEIRS model based on the SIR model by considering software diversity [25]. Li et al. investigated the influence of quarantine strategies on the spread of epidemics and proposed the SIQRS model based on the SIR model [26]. Huang et al. proposed a new-SQIRS epidemic model with demographics and vaccination [27]. Hosseini et al. proposed a SEIRS-V model with a vaccination state based on a rumor spreading model [28]. By similarly considering vaccinations and quarantine states, Hosseini et al. proposed the SEIRS-QV model [29].

These newer models further develop the understanding of network information propagation mechanisms. However, for the cases of preferential information propagation in Weibo networks, new challenges arise. Weibo is a vast online social network in China. According to the 2018 Weibo user development report, by the end of 2018, Weibo had more than 462 million monthly active users (MAU) and approximately 200 million daily active users (DAU). In Weibo, there are 47,300 super spreaders who have more than 500,000 followers, contributing to the super spreaders' great influence on their followers. Super spreaders publish information preferential to their followers, who may then forward it to other users who may not currently be a follower of the super spreader. Considering this huge influence of super spreaders, Zhang et al. established a super spreaders model to study public opinion and authoritative news, wherein the mean-field equations of super-rumor spreaders and super-authoritative spreaders were adopted [30]. Liu et al. also introduced the super spreader in the SAIR model [31]. Further to the impact from super spreaders, users have a hesitation state after they receive information from Weibo [32]; that is, users commonly wait for a variable amount of time before deciding whether or not to forward the preferential information. To account for this, the proposed method names users who have received the preferential information "lurker users".

This paper proposes the susceptible-lurker-super-normal-recovered (SEAIR) dynamics model to address preferential information propagation in Weibo. Both a super spreader compartment and a lurker compartment are adopted in the proposed SEAIR model, and entry to and exit from all five compartments are allowed. This more realistically reflects circumstances in Weibo, where individuals' information dissemination contribution status continuously changes.

The remainder of this paper is structured as follows. Section 2 briefly introduces the conventional SIR model followed by the proposed SEAIR model with entry and exit, lurker state, and super spreader state. Section 3 presents mathematical analysis of the SEAIR model, derivation of the basic reproductive ratio, and a proof of the global and local stability at the information-free equilibrium point. Section 4 compares the SEAIR model with the SIR model, discusses simulation results from real advertising message propagation data, and presents simulation analysis of SEAIR parameters.

2. SEAIR model

2.1. SIR model principles

The SIR model is a classic deterministic compartment model in which the entire population is divided into the following compartments [3]:

- Susceptible (S) compartment: the part of the group that is not infected but is susceptible to infection.
- Infectious (I) compartment: the part of the group that is infected by a disease.

Fig. 1. Transmission structure of the SIR model.

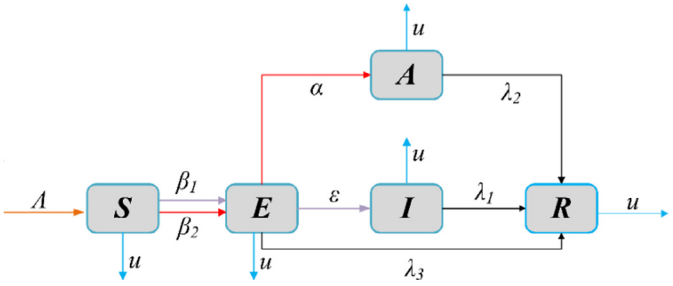

Fig. 2. Transmission structure diagram of the SEAIR model with entry and exit.

- Recovered (R) compartment: the part of the group that recovers from a disease or dies.

When an individual in the *S* compartment makes contact with an individual in the *I* compartment, the individual in the *S* compartment will be infected according to a certain probability, and is thus moved to the *I* compartment. When an individual is in the *I* compartment, they can be treated according to a certain probability, at which point individuals will either have immunity to the disease or die of the disease. In either case they move to the *R* compartment.

The dynamic performance of information dissemination is very similar to the spread of a disease: a sponsor publishes a raw forwarding and a large number of users, who are interested in this type of information (initially the sponsors' followers or followers of their followers), are affected to forward this forwarding. This is analogous to infection by a disease. These affected users continue to influence other users by sharing the information, akin to spreading a disease. After a period, affected users may lose interest in this information and cease to share it, akin to recovery from a disease. Therefore, users with general information interests in the online social network can be distinguished as susceptible users, infectious users or spreaders, and recovered users in the process of information dissemination, as described by the SIR model in Fig. 1.

The principles of the SIR model can be described by the mean-field equations as follows:

$$\frac{dS(t)}{dt} = -\frac{\beta \bar{k} S(t) I(t)}{N(t)} \tag{1}$$

$$\frac{dI(t)}{dt} = \frac{\beta \bar{k} S(t) I(t)}{N(t)} - \gamma I(t) \tag{2}$$

$$\frac{dR(t)}{dt} = \gamma I(t) \tag{3}$$

$$S(t) + I(t) + R(t) = N(t) \tag{4}$$

Here $S(t)$, $I(t)$, $R(t)$, and $N(t)$ represent the number of susceptible users, communicators, immune users and the general users in the network at time t, respectively. Simultaneously, the three initial values are non-negative, and the sum of $N(t)$ is an invariant. Moreover, $\bar{k}$ denotes the average of the nodes in the I compartment, which represents the number of followers or potential users to which information may be forwarded. β represents the rate at which a user is infected at each moment and γ represents the ratio of immunity.

2.2. SEAIR information dissemination characteristics

The phenomenon of super spreading is common in both epidemic spreads and information disseminations. Super spreaders have a greater influence on their followers (or followers in general) than normal spreaders. Hence, it is necessary to divide the spreaders of the online social network into super spreaders and normal spreaders. As an extension of the foundational SIR model [3], a super spreaders compartment A is thus needed. In most cases, susceptible users could think about the received information or wait for further related information before they decide to spread it. To reflect this hesitation, a lurker users compartment E is also needed. Incorporating these two new compartments into the SIR model results in the SEAIR model. The transmission structure diagram of the SEAIR model is shown in Fig. 2.

The SEAIR model is divided into five compartments:

- S denotes the susceptible users who are easily infected by outside information.
- E denotes the lurker users who may be converted to super spreaders, normal spreaders, or recovered users.
- I denotes the normal spreaders who have relatively limited efficiency for information dissemination.
- A denotes the super spreaders who have a higher efficiency for information dissemination.
- R denotes the recovered users who stop spreading the information or those who are not interested in the information from the beginning.

The rules of the SEAIR model can be summarized as follows:

(1) If the susceptible user receives the information from a normal spreader, the user is converted to a lurker user with probability β_1, where β_1 denotes the infection rate of normal spreaders. Generally, a normal spreader can spread the information to a friend and infect them.

(2) If the susceptible user receives the information from a super spreader, the user is converted to a lurker user with probability β_2, where β_2 denotes the infection rate of super spreaders. Usually, the followers of a super spreader are easily infected by the information spread by the super spreader.

(3) After an incubation period, the lurker user may be converted to a normal spreader with probability ε, a super spreader with probability α, or a recovered user if the information active period, $1/\lambda_3$, has expired. Thus, the lurker user decides to either spread the information as a normal spreader, spread it as a super spreader, or to not spread it.

(4) Both normal spreaders and super spreaders have effective information propagation periods. When the information propagation period is over, normal spreaders and super spreaders are converted to recovered users. This reflects the diminishing likelihood that information will be spread as time since its publication increases. Here, $1/\lambda_2$ denotes the information propagation period from the super spreader state to the recovered user, and $1/\lambda_1$ denotes the information propagation period from the normal spreader state to the recovered user.

(5) Let Λ denote the number of new users that are converted to susceptible users. It is common for a social network user to subscribe and unsubscribe to some topics, and to follow and unfollow certain super spreaders. Let u denote the probability of users in the five compartments who leave the information propagation progress. That is, in every state of the SEAIR model, people may detach from the model.

2.3. SEAIR dynamic equations

The notations used in the dynamic equations are defined as follows:

- $N(t)$: total number of users in the information dissemination network at time t.
- $S(t)$: number of susceptible users at time t and $S(t) \geq 0$.
- $E(t)$: number of lurker users at time t and $E(t) \geq 0$.
- $A(t)$: number of super spreaders at time t and $A(t) \geq 0$.
- $I(t)$: number of normal spreaders at time t and $I(t) \geq 0$.
- $R(t)$: number of recovered users at time t and $R(t) \geq 0$.

The SEAIR model can then be described by the following mean-field equations:

$$\frac{dS(t)}{dt} = \Lambda - \frac{\beta_1 \overline{k_1} S(t) I(t)}{N(t)} - \frac{\beta_2 \overline{k_2} S(t) A(t)}{N(t)} - uS(t), \tag{5}$$

$$\frac{dE(t)}{dt} = \frac{\beta_1 \overline{k_1} S(t) I(t)}{N(t)} + \frac{\beta_2 \overline{k_2} S(t) A(t)}{N(t)} - \varepsilon E(t) - \alpha E(t) - \lambda_3 E(t) - uE(t), \tag{6}$$

$$\frac{dI(t)}{dt} = \varepsilon E(t) - \lambda_1 I(t) - uI(t), \tag{7}$$

$$\frac{dA(t)}{dt} = \alpha E(t) - \lambda_2 A(t) - uA(t), \tag{8}$$

$$\frac{dR(t)}{dt} = \lambda_2 A(t) + \lambda_1 I(t) + \lambda_3 E(t) - uR(t), \quad \text{and} \tag{9}$$

$$S(t) + E(t) + I(t) + A(t) + R(t) = N(t). \tag{10}$$

Similar to the SIR model, the values of $S(t)$, $E(t)$, $A(t)$, $I(t)$, and $R(t)$ are not less than zero during the information propagation process. $\overline{k_1}$ and $\overline{k_2}$ are the average out-degree of the users in the I compartment and the A compartment, respectively. The definition of averaging out-degree $\overline{k_1}$ and $\overline{k_2}$ are different than the fine-grained classes used in modeling dynamics of complex socio-technical systems [33].

As described by Eqs. (5)–(10), the SEAIR model degenerates into an SIR model if Λ, β_2, u, λ_2, λ_3, and α are set to zero. By adding Eqs. (5)–(10) the following equation is obtained:

$$\frac{dN(t)}{dt} = \Lambda - uN(t). \tag{11}$$

In order to simplify the complexity of the model, this model $\Lambda = uN(t)$ is taken; therefore,

$S(t)+E(t)+I(t)+A(t)+R(t)=N(t)$, where $N(t)$ is a constant value in this model and is normalized to one. Then,

$$S(t)+E(t)+I(t)+A(t)+R(t)=1. \tag{12}$$

Hence, the feasible region for the SEAIR model is $U=\{S(t)\geq 0, E(t)\geq 0, A(t)\geq 0, I(t)\geq 0, R(t)\geq 0 \mid S(t)+E(t)+A(t)+I(t)+R(t)=1, t\geq 0\}$. It is thus sufficient to study the model dynamics of Eqs. (5)–(10) in U.

3. SEAIR dynamical analysis

In this section, the equilibrium point of the SEAIR model is calculated and the dynamic propagation characteristics of the model analyzed. The basic reproduction number of the model is also calculated and the local and global stability of the model at the information-free equilibrium point discussed.

The steady state of the SEAIR model is as follows:

$$\frac{dS(t)}{dt}=0,\ \frac{dE(t)}{dt}=0,\ \frac{dA(t)}{dt}=0,\ \frac{dI(t)}{dt}=0,\ \frac{dR(t)}{dt}=0. \tag{13}$$

Hence, the equilibrium point of the model is the information-free equilibrium state $EQ_1=(1\ 0\ 0\ 0\ 0)$ and endemic stage $EQ_2=(S^*\ E^*\ A^*\ I^*\ R^*)$, where

$$S^*=\frac{u}{u+(\beta_1\overline{k_1}+\frac{\alpha(\lambda_{1+}u)\beta_2\overline{k_2}}{\varepsilon(\lambda_2+u)})I^*},\quad E^*=\frac{\lambda_{1+}u}{\varepsilon}I^*,\quad A^*=\frac{\alpha(\lambda_{1+}u)}{\varepsilon(\lambda_2+u)}I^*,$$

$$R^*=\frac{\lambda_2\alpha(\lambda_{1+}u)+\lambda_1\varepsilon(\lambda_2+u)+\lambda_3(\lambda_{1+}u)(\lambda_2+u)}{\varepsilon u(\lambda_2+u)}I^*$$

$$\text{and}\quad I^*=\frac{u\varepsilon^2(\lambda_2+u)\beta_1\overline{k_1}+u\varepsilon\alpha(\lambda_{1+}u)\beta_2\overline{k_2}-(\varepsilon+\alpha+\lambda_3+u)(\lambda_{1+}u)(\lambda_2+u)\varepsilon u}{(\varepsilon+\alpha+\lambda_3+u)[\varepsilon(\lambda_2+u)\beta_1\overline{k_1}+\alpha(\lambda_{1+}u)\beta_2\overline{k_2}](\lambda_{1+}u)}.$$

3.1. Basic reproductive ratio

Mathematical epidemiology often involves the determination of the threshold size of a model. The size of the threshold determines whether the infectious state can always exist in the network. This threshold is also known as the basic reproductive ratio $\mathcal{R}_0$. $\mathcal{R}_0$ represents the expected value of a typical infection in a complete susceptible population [34]. In general, the basic reproductive ratio examines the global dynamics of the model. It is derived from a locally stable information-free equilibrium and serves as a threshold to control the dynamics of information dissemination [35]. If $\mathcal{R}_0<1$, an average infectious individual transmits to less than one individual during its entire transmission cycle, and the dissemination of information thus disappears or fades away from the network. If instead $\mathcal{R}_0>1$, the average individual in the network infects more than one individual in its propagation cycle, such that information dissemination persists in the network [35].

The basic propagation number is generally obtained by calculating the spectral radius of the next generation matrix of the model. Let $x=(E\ I\ A\ S\ R)^{\mathrm{T}}$, then Eqs. (5)–(10) can be rewritten as follows:

$$\dot{x}=\mathcal{F}-\mathcal{V}, \tag{14}$$

where

$$\mathcal{F}=\begin{pmatrix}\frac{\beta_1\overline{k_1}S(t)I(t)}{N(t)}+\frac{\beta_2\overline{k_2}S(t)A(t)}{N(t)}\\0\\0\\0\\0\end{pmatrix}\quad\text{and}\quad\mathcal{V}=\begin{pmatrix}\varepsilon E(t)+\alpha E(t)+\lambda_3E(t)+uE(t)\\-\varepsilon E(t)+\lambda_1I(t)+uI(t)\\-\alpha E(t)+\lambda_2A(t)+uA(t)\\-\Lambda+\frac{\beta_1\overline{k_1}S(t)I(t)}{N(t)}+\frac{\beta_2\overline{k_2}S(t)A(t)}{N(t)}+uS(t)\\-\lambda_2A(t)-\lambda_1I(t)-\lambda_3E(t)+uR(t)\end{pmatrix}.$$

For the E, I, and A compartments, there is $x_0=(0\ 0\ 0\ S_0\ R_0)^{\mathrm{T}}$ when $E=I=A=0$, the equilibrium point. From Eq. (12), $N(t)=1$ so that $S_0=1, R_0=0$ is an equilibrium point.

F and V are taken as a 3×3 matrix [36],

$$F=\begin{pmatrix}0&\frac{\beta_1\overline{k_1}S(t)}{N(t)}&\frac{\beta_2\overline{k_2}S(t)}{N(t)}\\0&0&0\\0&0&0\end{pmatrix},\quad V=\begin{pmatrix}\alpha+u+\varepsilon+\lambda_3&0&0\\-\varepsilon&\lambda_1+u&0\\-\alpha&0&\lambda_2+u\end{pmatrix},$$

to obtain:

$$V^{-1}=\frac{1}{(\alpha+u+\varepsilon+\lambda_3)(\lambda_1+u)(\lambda_2+u)}$$

$$* \begin{pmatrix} (\lambda_1+u)(\lambda_2+u) & 0 & 0 \\ \varepsilon(\lambda_2+u) & (\alpha+u+\varepsilon+\lambda_3)(\lambda_2+u) & 0 \\ \alpha(\lambda_1+u) & 0 & (\alpha+u+\varepsilon+\lambda_3)(\lambda_1+u) \end{pmatrix}.$$

The spectral radius is calculated as,

$$\rho\left(FV^{-1}\right) = \frac{1}{(\alpha+u+\varepsilon+\lambda_3)(\lambda_2+u)(\lambda_1+u)} * \begin{pmatrix} \varepsilon(\lambda_2+u)\frac{\beta_1\overline{k_1}S(t)}{N(t)} + \alpha(\lambda_1+u)\frac{\beta_2\overline{k_2}S(t)}{N(t)} & (\alpha+u+\varepsilon+\lambda_3)(\lambda_2+u)\frac{\beta_1\overline{k_1}S(t)}{N(t)} & (\alpha+u+\varepsilon+\lambda_3)(\lambda_1+u)\frac{\beta_2\overline{k_2}S(t)}{N(t)} \\ 0 & 0 & 0 \\ 0 & 0 & 0 \end{pmatrix},$$

and

$$\Re_0 = \rho\left(FV^{-1}\right) = \frac{(\varepsilon(\lambda_2+u)\frac{\beta_1\overline{k_1}S(t)}{N(t)} + \alpha(\lambda_1+u)\frac{\beta_2\overline{k_2}S(t)}{N(t)})}{(\alpha+u+\varepsilon+\lambda_3)(\lambda_2+u)(\lambda_1+u)}. \tag{15}$$

Thus, when $N(t)=1$ and $S_0=1$,

$$\Re_0 = \frac{(\varepsilon(\lambda_2+u)\beta_1\overline{k_1} + \alpha(\lambda_1+u)\beta_2\overline{k_2})}{(\alpha+u+\varepsilon+\lambda_3)(\lambda_2+u)(\lambda_1+u)}. \tag{16}$$

3.2. Information-free equilibrium stability analysis

The stability of the information-free equilibrium of the model of Eqs. (5)–(8) is investigated to study the dynamical behaviors of the SEAIR model. According to Eqs. (5)–(8), the Jacobian matrix obtains,

$$J = \begin{bmatrix} -\frac{\beta_1\overline{k_1}I(t)}{N(t)} - \frac{\beta_2\overline{k_2}A(t)}{N(t)} - u & 0 & -\frac{\beta_1\overline{k_1}S(t)}{N(t)} & -\frac{\beta_2\overline{k_2}S(t)}{N(t)} \\ \frac{\beta_1\overline{k_1}I(t)}{N(t)} + \frac{\beta_2\overline{k_2}A(t)}{N(t)} & -\varepsilon-\alpha-\lambda_3-u & \frac{\beta_1\overline{k_1}S(t)}{N(t)} & \frac{\beta_2\overline{k_2}S(t)}{N(t)} \\ 0 & \varepsilon & -\lambda_1-u & 0 \\ 0 & \alpha & 0 & -\lambda_2-u \end{bmatrix}. \tag{17}$$

The Jacobian matrix at the information-free equilibrium EQ_1 is

$$\mathrm{J}\ (EQ_1) = \begin{bmatrix} -u & -\varepsilon-\alpha-\lambda_3-u & 0 & 0 \\ 0 & -\varepsilon-\alpha-\lambda_3-u & 0 & a_1 \\ 0 & 0 & -\lambda_1-u & \frac{\varepsilon(\lambda_2+u)}{\alpha} \\ 0 & 0 & 0 & a_2 \end{bmatrix},$$

where

$$a_1 = \frac{\beta_2\overline{k_2}\alpha(-\lambda_1-u) - \beta_1\overline{k_1}\varepsilon(\lambda_2+u)}{\alpha(-\lambda_1-u)}, \text{ and}$$

$$a_2 = -\frac{\beta_1\overline{k_1}\varepsilon(\lambda_2+u) + \beta_2\overline{k_2}\alpha(\lambda_1+u) - (\alpha+u+\varepsilon+\lambda_3)(\lambda_2+u)(\lambda_1+u)}{(\alpha+u+\varepsilon+\lambda_3)(\lambda_1+u)}.$$

The Eigen function of $J(EQ_1)$ is

$$|\lambda E - J(EQ_1)| = \begin{bmatrix} \lambda+u & 0 & 0 & a_1 \\ 0 & \lambda+\varepsilon+\alpha+\lambda_3+u & 0 & -a_1 \\ 0 & 0 & \lambda+\lambda_{1+}u & -\frac{\varepsilon(\lambda_2+u)}{\alpha} \\ 0 & 0 & 0 & \lambda+a_2 \end{bmatrix}.$$

Matrix E is the identity matrix, and λ is the eigenvalue.
Thus, the Eigen function of $J(EQ_1)$ is equal to $f(\lambda) = b_4\lambda^4 + b_3\lambda^3 + b_2\lambda^2 + b_1\lambda^1 + b_0$, where

$$\begin{aligned} b_4 &= 1, \\ b_3 &= (\varepsilon+\alpha+\lambda_3+3u+\lambda_1+\mathrm{a}_2), \\ b_2 &= u(\varepsilon+\alpha+\lambda_3+2u+\lambda_1+\mathrm{a}_2) + (\varepsilon+\alpha+\lambda_3+u)(\lambda_1+u+\mathrm{a}_2) + \mathrm{a}_2(\lambda_1+u), \\ b_1 &= \mathrm{u}[(\varepsilon+\alpha+\lambda_3+u)(\lambda_1+u) + \mathrm{a}_2(\lambda_1+u) + \mathrm{a}_2(\varepsilon+\alpha+\lambda_3+u)] \end{aligned} \tag{18}$$

$$+ a_2 (\varepsilon + \alpha + \lambda_3 + u)(\lambda_1 + u),$$
$$b_0 = u(\varepsilon + \alpha + \lambda_3 + u)(\lambda_1 + u) a_2.$$

The following lemma and theorems are used in the stability analysis of the model (Theorems 1 and 2 are based on existing works on stability analysis [28,37]).

Theorem 1. *If $\Re_0 \leq 1$ the information-free equilibrium EQ_1 is locally asymptotically stable, and it is unstable if $\Re_0 > 1$. $\Re_0$ is calculated by Eq. (16).*

Proof. Base on the Routh–Hurwitz criterion, the Routh–Hurwitz array for information-free equilibrium EQ_1 is as follows:

$$\begin{bmatrix} b_4 & b_2 & b_0 \\ b_3 & b_1 & 0 \\ c_1 & b_0 & 0 \\ d_1 & 0 & 0 \\ b_0 & 0 & 0 \end{bmatrix}, \tag{19}$$

where $c_1 = \frac{b_3 b_2 - b_4 b_1}{b_3}$, and $d_1 = \frac{b_1 c_1 - b_3 b_0}{c_1}$.

According to the theorem in [38], the stability of the system necessitates that all elements of the first column of the dynamic Routh array must have positive values. Hence, the stability of the model necessitates that $b_4 > 0$, $b_3 > 0$, $c_1 > 0$, $d_1 > 0$ and $b_0 > 0$. When $\Re_0 < 1$, it can be proven by Eq. (18) that $b_4 > 0$, $b_3 > 0$, $b_1 > 0$ and $b_0 > 0$ if $b_3 b_2 > b_4 b_1$, then $c_1 > 0$.

Furthermore, when $b_1 c_1 > b_3 b_0$, then $d_1 > 0$. Then, $b_4 > 0$, $b_3 > 0$, $b_1 > 0$, and $b_0 > 0$. The condition that the first column coefficient of the Routh array is greater than zero can be presented as $b_3 b_2 > b_4 b_1$ and $b_1 c_1 > b_3 b_0$. Thus, the Routh–Hurwitz stability conditions are satisfied, which implies that the information-free equilibrium is locally asymptotically stable.

Theorem 2. *When $\Re_0 \leq 1$, the information-free equilibrium EQ_1 is globally asymptotically stable, and it is unstable when $\Re_0 > 1$.*

Proof. The eigenvalue of the $J(EQ_1)$ matrix is $\lambda = -u$, $\lambda = -\varepsilon - \alpha - \lambda_3 - u$, $\lambda = -\lambda_1 - u$ or $\lambda = -a_2$, which is obtained by the characteristic equation $(\lambda + u)(\lambda + \varepsilon + \alpha + \lambda_3 + u)(\lambda + \lambda_1 + u)(\lambda + a_2) = 0$.

When $\Re_0 \leq 1$, then $a_2 \geq 0$. Moreover, $a_2 = 0$ if and only if $\Re_0 = 1$. Thus, when $\Re_0 < 1$, the eigenvalue of $J(EQ_1)$ matrix is less than zero. If and only if $\Re_0 > 1$, there is a unique positive eigenvalue λ of the $J(EQ_1)$ matrix. According to the Perron–Frobenius theorem, it is suggested that maximal real part of all eigenvalues of the $J(EQ_1)$ matrix is greater than zero only if $\Re_0 > 1$. Thus, when $\Re_0 > 1$, the eigenvalues of the $J(EQ_1)$ matrix include three negative eigenvalues and one positive eigenvalue. Accordingly, EQ_1 is an unstable saddle point in this case.

It can be obtained that $\varepsilon \frac{\beta_1 \overline{k_1}}{\lambda_1 + u} + \alpha \frac{\beta_2 \overline{k_2}}{\lambda_2 + u} \leq \alpha + u + \varepsilon + \lambda_3$ by Eq. (16), when $\Re_0 \leq 1$. Assuming that there exist a and b that satisfy the condition $a + b \leq \alpha + u + \varepsilon + \lambda_3$, the corresponding a and b can be found such that $\varepsilon \frac{\beta_1 \overline{k_1}}{\lambda_1 + u} \leq a$ 和 $\alpha \frac{\beta_2 \overline{k_2}}{\lambda_2 + u} \leq b$. According to the Li–Muldowney linear Lyapunov function, the following Lyapunov function for the model is constructed:

$$V(t) = E(t) + \frac{b}{\alpha} A(t) + \frac{a}{\varepsilon} I(t). \tag{20}$$

The time derivative of V (t) along the solution of the model of Eqs. (6)–(8) is calculated as follows: $\frac{dV(t)}{dt} = \beta_1 \overline{k_1} S(t) I(t) + \beta_2 \overline{k_2} S(t) A(t) - (\varepsilon + \alpha + \lambda_3 + u) E(t) + bE(t) - \frac{b(\lambda_2 + u) A(t)}{\alpha} + aE(t) - \frac{a(\lambda_1 + u) I(t)}{\varepsilon}$,

$$\frac{dV(t)}{dt} = \left(\beta_1 \overline{k_1} S(t) - \frac{a(\lambda_1 + u)}{\varepsilon}\right) I(t) + (\beta_2 \overline{k_2} S(t) - \frac{b(\lambda_2 + u)}{\alpha}) A(t) + [b + a - (\varepsilon + \alpha + \lambda_3 + u)] E(t).$$

When $\Re_0 \leq 1$, then $\frac{dV(t)}{dt} \leq 0$. Moreover, $\frac{dV(t)}{dt} = 0$ is only available under certain circumstances. Therefore, the information-free equilibrium EQ_1 (1 0 0 0 0) is globally asymptotically stable.

4. Simulations and results discussion

4.1. Real case data, model parameters, and simulation network structure

To verify the SEAIR model, data were collected from a Baidu App promotional advertisement in Weibo [39]. The promotional activity affected a large number of users, generating 336,298 reposts. Fig. 3(a) shows the real cumulative

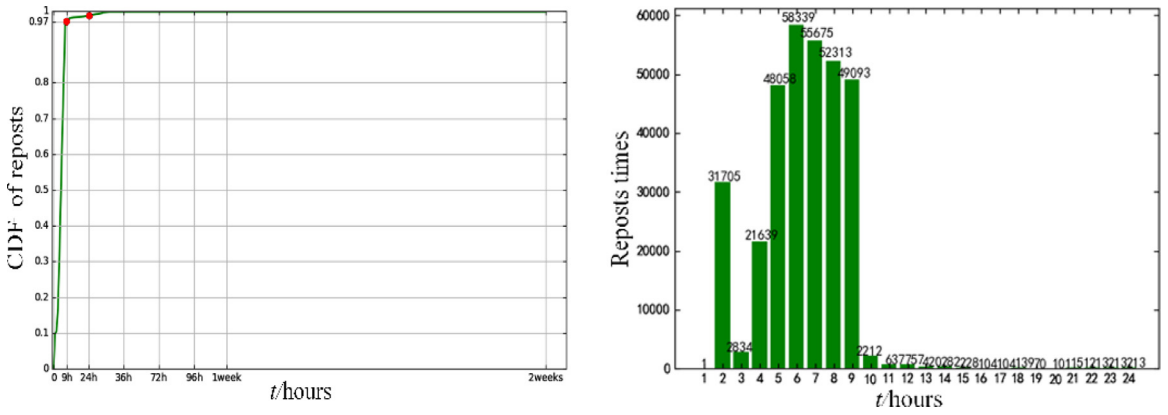

(a) CDF of the number of reposts (b) Number of reposts within the first 24 hours

Fig. 3. Case data collected from the Baidu App promotional advertisement in Weibo.

Table 1
Parameter ranges of SEAIR and SIR models.

Model	Parameter	Range	Default value
SEAIR	$\overline{k_1}$	[1, 232]	3.3
	$\overline{k_2}$	[10, 10 000]	575
	α	(0, 1)	0.01
	ε	(0, 1)	0.8
	β_1	(0, 1)	0.5
	β_2	(0, 1)	0.5
	λ_1	(0, ∞)	1
	λ_2	(0, ∞)	2
	λ_3	(0, ∞)	2
	Λ	(0, ∞)	$0.1 \times N(t)$
	u	(0, 1)	0.1
SIR	$\overline{k}$	[1, 500]	20.1
	β	(0, 1)	0.2
	γ	(0, ∞)	2

distribution function (CDF) of the repost number. The CDF results indicate that the process of advertisement reposts occurred primarily in the first day. Within the first 24 h, 325,717 reposts were generated, which was approximately 96.9% of the total reposts. The number of reposts per hour of the Baidu App promotional advertisement is shown in Fig. 3(b).

To select suitable parameters for the SEAIR model and the conventional SIR model, the mean square error was calculated, as shown in Eq. (21):

$$MSE = \frac{1}{n}\sum_{1}^{n} |I(t) - \hat{I}(t)|^2 \tag{21}$$

where $\hat{I}(t)$ is the fitted value of $I(t)$ (the observed values) at time t, and n is the number of observations. The parameter ranges of the SEAIR model and the SIR model are shown in Table 1.

Additionally, to simulate the networking connection of a social network, the Barabási–Albert (BA) network structure was adopted. Fig. 4(a) shows a simulation network including 1000 nodes with an average degree of 3.3. The degree distribution of each node in Fig. 4(a) is shown in Fig. 4(b), with sufficient scale-free features. Hence, the adopted BA network structure was feasible [2,20,30]. Fig. 4(c) shows the degree distribution map of 600,000 nodes generated by this network, which presents an approximate power regular distribution. The degree of distribution also showed that most of the users in the network had little influence on other users; most of the users were affected by a small number of special users. This is similar to the situation in Weibo. Additionally, according to the generated degree distribution, 0.00633% of the entire nodes were distinguished as super spreader nodes. This informed the selection of $\overline{k_1} = 3.31$, $\overline{k_2} = 575$, and $\overline{k} = 20.1$, according to the total number of normal spreaders.

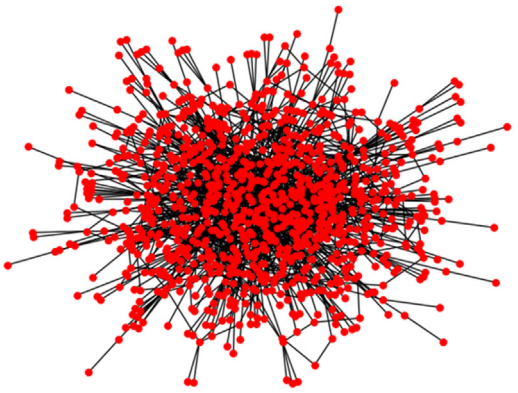

(a) Simulation network diagram with 1000 nodes

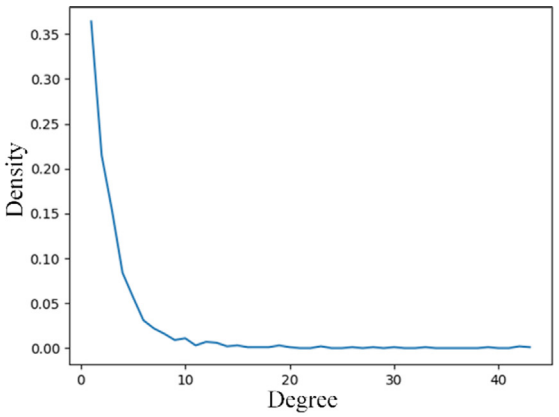

(b) Degree distribution of the 1000 nodes

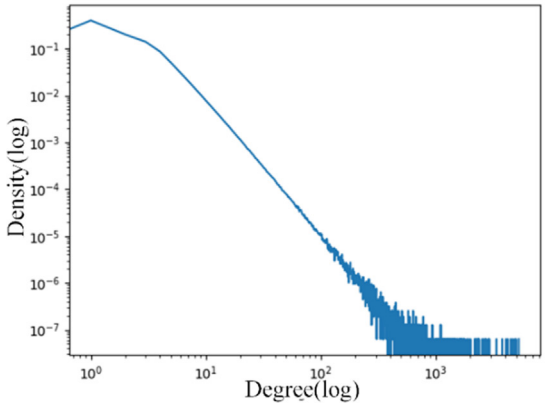

(c) Degree distribution of the 600,000-node network

Fig. 4. Topology of the simulation network and the degree distribution. The 1000-node simulation network is an example to illustrate the BA network.

4.2. Performance of the SIR and SEAIR models

With the case data collected from the Baidu App promotional advertisement in Weibo (Fig. 3(b)), the parameter fitting of the SEAIR model was made with a Python programmed numerical method. The parameters were varied at a fixed step size of 0.001, and the root mean square error (RMSE) of $I(t)$ was calculated according to Eq. (22) at each step. Finally, the optimal value of the parameters with the least RMSE was selected.

$$RMSE = \sqrt{\frac{1}{n} \times \sum_{1}^{n} |I(t) - \hat{I}(t)|^2} \tag{22}$$

The SIR model described by Eqs. (1)–(4) was simulated. The optimized parameters of the SIR model were $\overline{k} = 20.1$, $\beta = 0.207$, and $\lambda = 2.15$. The initial states of the SIR model were $S(0) = 599999$, $I(0) = 1$ and $R(0) = 0$. Fig. 5 shows the dynamic change process of the number of reposts in $S(t)$, $I(t)$, and $R(t)$ in the simulation network.

Additionally, the simulated $I(t)$ of the SIR model was compared with the case data collected from the activity of the Baidu App promotional advertisement in the first 20 h. As shown in Fig. 6, this exhibited a fairly large curve-fitting error.

Next, the SEAIR model described by Eqs. (5)–(10) was simulated. The optimized parameters of the SEAIR model were $\overline{k_1} = 3.3$, $\overline{k_2} = 575$, $\beta_1 = 0.451$, $\beta_2 = 0.528$, $\alpha = 0.081$, $\varepsilon = 0.883$, $u = 0.021$, $\lambda_1 = 0.51$, $\lambda_2 = 2.39$, and $\lambda_3 = 2.59$. The initial states of the SEAIR model were $S(0) = 599999$, $E(0) = 0$, $A(0) = 1$, $I(0) = 0$, $R(0) = 0$. Fig. 7 shows the dynamic change process of number of reposts in $S(t)$, $E(t)$, $A(t)$, $I(t)$, and $R(t)$ in the simulation network.

Additionally, the simulated $I(t)$ and $A(t)$ of the SEAIR model were compared with the case data in the first 20 h. This exhibited a significantly reduced curve-fitting error (see Fig. 8).

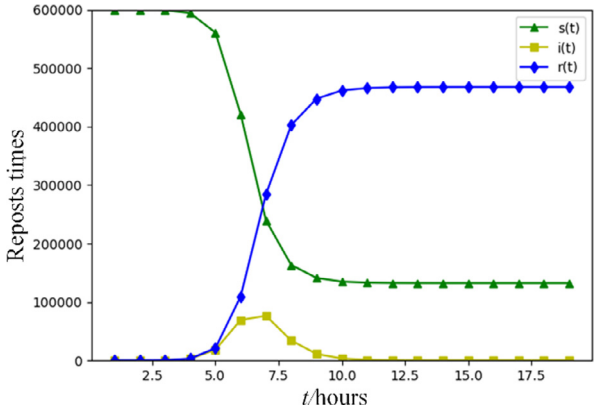

Fig. 5. Number of reposts dynamic change process in the SIR model with $\overline{k} = 20.1$, $\beta = 0.207$, and $\lambda = 2.15$.

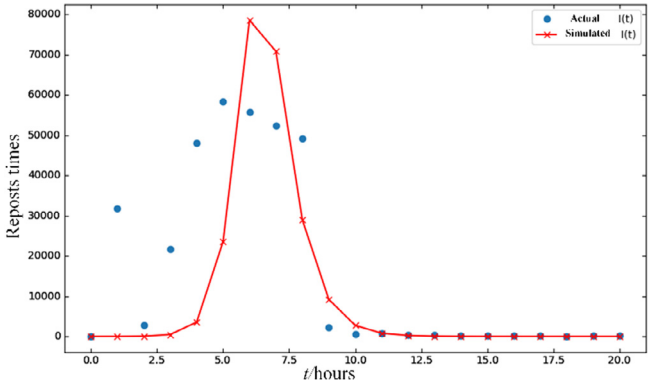

Fig. 6. Comparison of simulated $I(t)$ in the SIR model with case data.

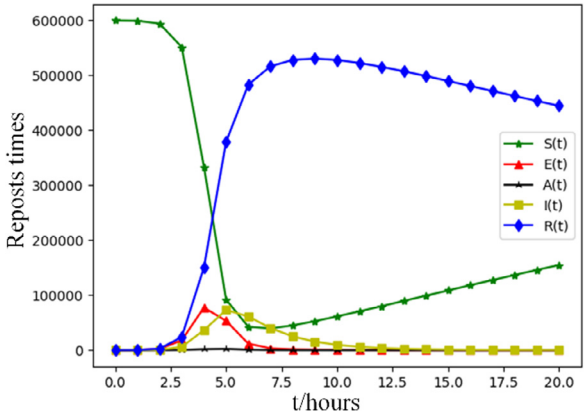

Fig. 7. Number of reposts dynamic change process in the SEAIR model with $\overline{k_1} = 3.3$, $\overline{k_2} = 575$, $\beta_1 = 0.451$, $\beta_2 = 0.528$, $\alpha = 0.081$, $\varepsilon = 0.883$, $u = 0.021$, $\lambda_1 = 0.51$, $\lambda_2 = 2.39$, $\lambda_3 = 2.59$, and $\mathcal{R}_0 = 3.545$.

Table 2
Comparison of RMSE and MAE of SIR and SEAIR.

Model	RMSE	MAE
SIR	16 868	9848
SEAIR	11 265	7412

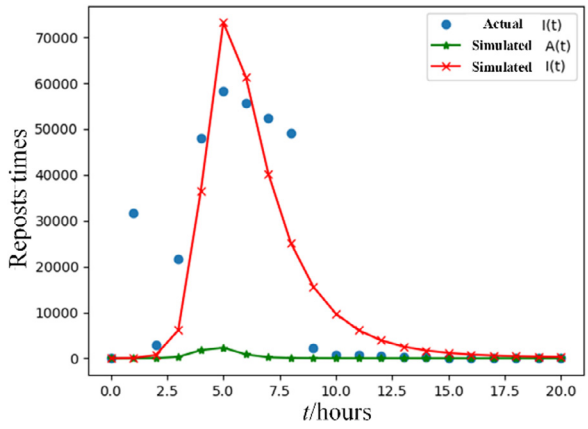

Fig. 8. Comparison of the case data with $I(t)$ and $A(t)$ in the SEAIR model.

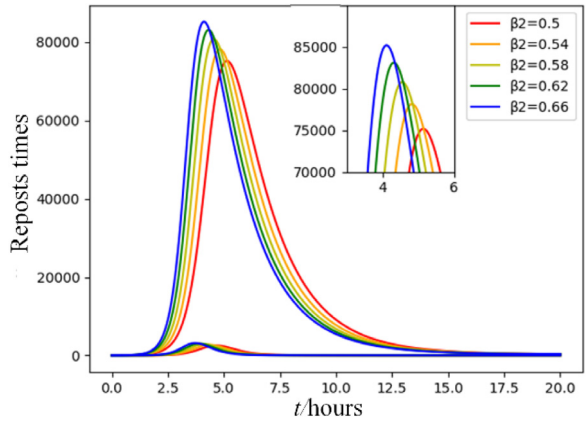

Fig. 9. Number of reposts of normal spreaders $I(t)$ and super spreaders $A(t)$ with various super spreader infection rates β_2.

Table 2 lists the RMSE and average absolute error (Eq. (23)), of the simulated results of the SIR and SEAIR model compared with the actual data in the first 20 h. Compared with the SIR model, the RMSE and MAE of the SEAIR model were less by 33.2% and 24.74%, respectively.

$$MAE = \frac{1}{n}\sum_{1}^{n}\left|I(t) - \hat{I}(t)\right| \tag{23}$$

4.3. Analysis of parameter performance of the SEAIR model

In the SEAIR model, parameters were utilized that related to super spreaders, normal spreaders, lurker users, and the exit rates of the five compartments. Hence, it is necessary to evaluate the parameters on the performance of the model. In this section, each parameter is analyzed separately, while other parameters are kept at the default value listed in Table 1.

(1) Super spreader parameters

Parameter β_2 denotes the infection rate of the super spreaders. As shown in Fig. 9, as β_2 increased, the growth rate of both the normal spreaders $I(t)$ (the upper curves) and the super spreaders $A(t)$ (the lower curves) increased. Additionally, the maximum number of reposts of $I(t)$ and $A(t)$ also increased. This suggests that super spreaders with high impact, such as official accounts, hasten the propagation process of information dissemination.

The super spreader conversion ratio α controlled the growth rate of the super spreaders involved in information dissemination. As shown in Fig. 10, as α increased, both the growth rate of the normal spreaders $I(t)$ (the upper curves) and the super spreaders $A(t)$ (the lower curves) increased. The maximum number of reposts of $I(t)$ and $A(t)$ also increased. This suggests that when more super spreaders are involved in information dissemination, more normal spreaders and other super spreaders are affected. The small graph in Fig. 10 is an enlarged view of the $I(t)$ value between zero and 80. It can be seen that when α is equal to 0.008, the change in $I(t)$ has a declining trend from the very beginning. The $\mathcal{R}_0$

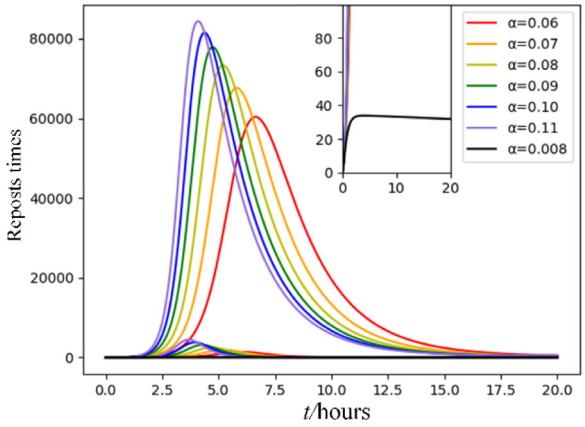

Fig. 10. Number of reposts of normal spreaders $I(t)$ and super spreaders $A(t)$ with various super spreader conversion ratios α.

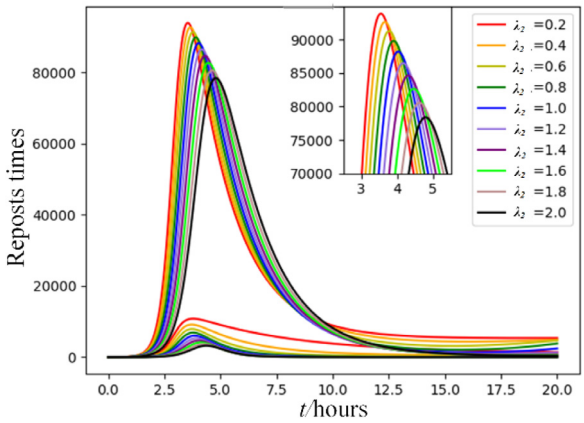

Fig. 11. Number of reposts of normal spreaders $I(t)$ and super spreaders $A(t)$ with various super spreader information propagation periods λ_2.

formula can find that its value is close to and less than one when α is equal to 0.008. Multiple experiments have found that when the $\mathcal{R}_0$ value is near one, the trend of $I(t)$ shows the same characteristics.

Parameter $1/\lambda_2$ denotes the information propagation period from a super spreader state to a recovered user state. As shown in Fig. 11, as λ_2 increased, both the growth rate of normal spreaders $I(t)$ (the upper curves) and super spreaders $A(t)$ (the lower curves) decreased. The maximum number of reposts of $I(t)$ and $A(t)$ also decreased. This suggests that when a super spreader focuses on the preferential information for a longer period, more normal spreaders and other super spreaders are affected.

According to the results from Figs. 9–11, the super spreader has a significant impact on the number of reposts of both normal spreaders $I(t)$ and other super spreaders $A(t)$. The super spreader can greatly expand the spread scope and spread speed of preferential information.

(2) Normal spreader parameters

Parameter β_1 denotes the infection ratio of normal spreaders. Similar to β_2, as β_1 increased, both the growth rate of normal spreaders $I(t)$ (the upper curves) and super spreaders $A(t)$ (the lower curves) increased (Fig. 12). However, the growth rate of $I(t)$ and $A(t)$ affected by β_1 is much lower than that by β_2. This signifies that normal spreaders have a weak impact on preferential information spread relative to super spreaders.

The increase in the conversion ratio ε of the normal spreader greatly increased the spread speed and spread scope of preferential information among normal spreaders $I(t)$ (the upper curves), as shown in Fig. 13. However, as ε increased, the number of reposts of super spreaders $A(t)$ (the lower curves) decreased. This suggests that super spreaders repost preferential information less when it has already been spread among normal spreaders.

As shown in Fig. 14, as λ_1 increased, the growth rate of normal spreaders $I(t)$ (the upper curves) greatly decreased. However, this had little impact on the change in the number of reposts of super spreaders $A(t)$ (the lower curves). This suggests that normal spreaders are more likely to repost preferential information with a longer spread period (e.g. hot topics).

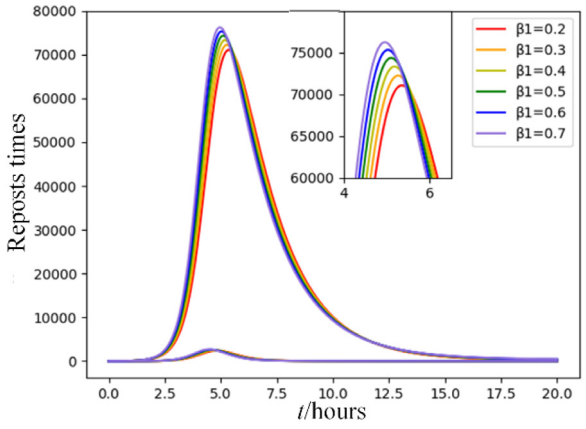

Fig. 12. Number of reposts of normal spreaders $I(t)$ and super spreaders $A(t)$ with various normal spreader infection rates β_1.

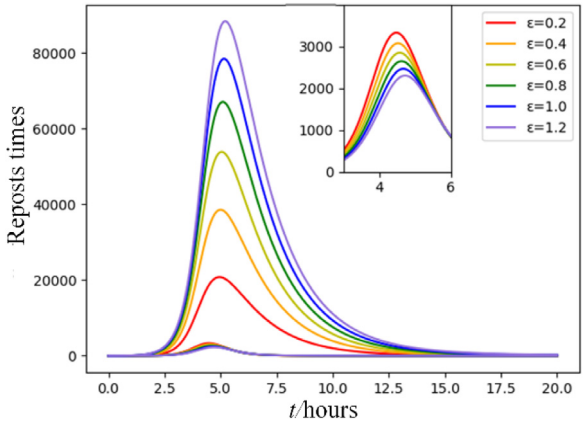

Fig. 13. Number of reposts of normal spreaders $I(t)$ and super spreaders $A(t)$ with various normal spreader conversion ratios ε.

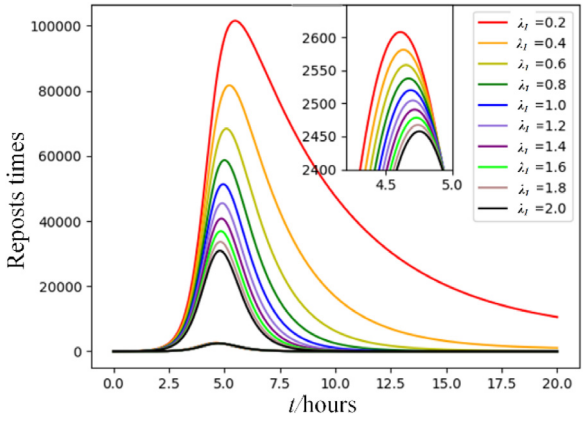

Fig. 14. Number of reposts of normal spreaders $I(t)$ and super spreaders $A(t)$ with various normal spreader information propagation periods λ_1.

According to the results from Figs. 12–14, normal spreaders affect the number of reposts of normal spreaders $I(t)$ but have a weaker influence on the spread scope and spread speed of the preferential information of super spreader. Additionally, normal spreaders have little impact on the number of reposts of super spreaders $A(t)$.

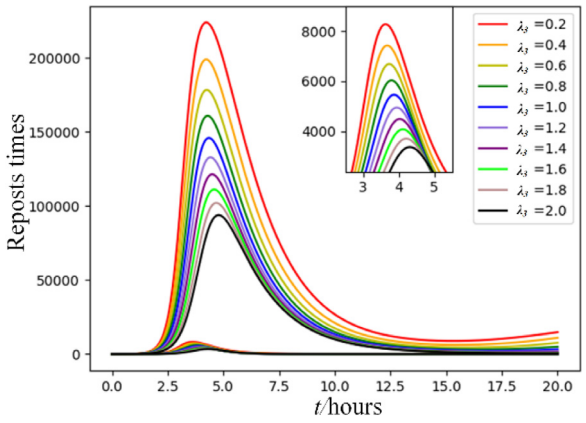

Fig. 15. Number of reposts of normal spreaders *I(t)* and super spreaders *A(t)* with various conversion ratios λ_3.

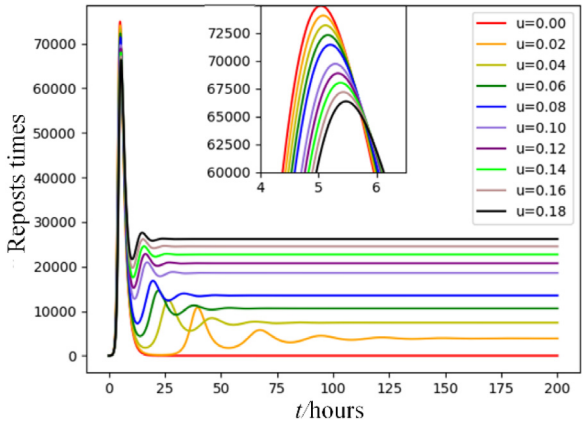

Fig. 16. Number of reposts of normal spreaders *I(t)* with various information propagation exit probabilities *u*.

(3) Lurkers and leaving rate parameters

Note that $1/\lambda_3$ denotes the information active period, after which period the lurker user becomes a recovered user. With increase in λ_3, the growth rate and maximum value of normal spreaders *I(t)* (the upper curves) and super spreaders *A(t)* (the lower curves) significantly decreased. It is reasonable that the number of reposts declines as more lurkers become recovered users (see Fig. 15).

As shown in Fig. 16, as *u* increases, the growth rate and maximum value of normal spreaders *I(t)* decreases. Reasonably, the number of reposts declines if people exit faster. The oscillating effect is also consistent with the low propagation tendencies of the night-time activity in real networks. Simultaneously, as *u* increases, the number of users in the susceptible state increases, which promotes the relatively high forwarding phenomenon in later stages.

5. Conclusion

In this paper, the SEAIR model, which consists of a super spreader compartment, a lurker compartment, and entry and exit capabilities for all compartments was proposed to address preferential information propagation in Weibo. The dynamic equations of the SEAIR model are proposed according to the mean-field theory. The decisive information propagation basic reproductive ratio $\mathcal{R}_0$ is obtained by calculating the spectral radius of the matrix FV^{-}. The number of users of the susceptible and recovered states are then determined by $\mathcal{R}_0$. Simulation results of a real case show that, compared with the SIR model, the RMSE and MAE of the SEAIR model were less by 33.2% and 24.74%, respectively. This verifies that the SEAIR model analyzes the dynamic process of preferential information propagation in Weibo more realistically than the SIR model does. The influence of parameters on the model's performance was also evaluated: super spreaders have a significant impact on the number of reposts of both normal spreaders and other super spreaders; contrastingly, normal spreaders can affect the number of reposts of primarily normal spreaders with a relatively weaker influence on the spread scope and spread speed of the preferential information. Future studies should collect more real cases regarding preferential information propagation in Weibo for further performance evaluations of the SEAIR model.

Additionally, in the proposed SEAIR model, user entry and exit rates are equivalent for modeling simplicity. However, in a real network they may often be unequal. Accordingly, in future work, entry and exit rate inequalities should be further investigated.

CRediT authorship contribution statement

Minglei Fu: Conceptualization, Data curation, Formal analysis, Funding acquisition, Writing - original draft. **Jun Feng:** Investigation, Methodology , Visualization, Writing - original draft. **Dmytro Lande:** Investigation, Methodology. **Oleh Dmytrenko:** Formal analysis, Methodology, Writing - review & editing. **Dmytro Manko:** Formal analysis, Methodology. **Ryhor Prakapovich:** Writing - review & editing.

Declaration of competing interest

The authors declare that they have no known competing financial interests or personal relationships that could have appeared to influence the work reported in this paper.

Acknowledgment

This work was funded by the National Natural Science Foundation of China [grant number 61973275]. We are also thankful for the financial support from the Innovative Talent Support Program of Yiwu city, China.

References

[1] C. Wan, T. Li, Z.H. Guan, Y. Wang, X. Liu, Spreading dynamics of an e-commerce preferential information model on scale-free networks, Phys. A 467 (2017) 192–200, http://dx.doi.org/10.1016/j.physa.2016.09.035.
[2] M. Fu, H. Yang, J. Feng, W. Guo, Z. Le, D. Lande, D. Manko, Preferential information dynamics model for online social networks, Phys. A 506 (2018) 993–1005, http://dx.doi.org/10.1016/j.physa.2018.05.017.
[3] M.E. Newman, Spread of epidemic disease on networks., Phys. Rev. E 66 (2002) 16128.
[4] T. Preis, H.S. Moat, H. Eugene Stanley, Quantifying trading behavior in financial markets using google trends, Sci. Rep. 3 (2013) 1–6, http://dx.doi.org/10.1038/srep01684.
[5] C. Curme, A. Avakian, H.S. Moat, T. Preis, H.E. Stanley, D.Y. Kenett, Quantifying Wikipedia usage Patterns before Stock Market Moves, Sci. Rep. 3 (2013) 1–5, http://dx.doi.org/10.1038/srep01801.
[6] A.L. Barabási, R. Albert, H. Jeong, Mean-field theory for scale-free random networks, Phys. A 272 (1999) 173–187, http://dx.doi.org/10.1016/S0378-4371(99)00291-5.
[7] A. Singh, R. Kumar, Y.N. Singh, Rumor Dynamics with acceptability Factor and Inoculation of Nodes in scale free Networks, in: 8Th Int. Conf. Signal Image Technol. Internet Based Syst. (Sitis 2012), 2012, pp. 798–804, http://dx.doi.org/10.1109/SITIS.2012.120.
[8] W. Liu, C. Liu, X. Liu, S. Cui, X. Huang, Modeling the spread of malware with the influence of heterogeneous immunization, Appl. Math. Model. 40 (4) (2016) 3141–3152, http://dx.doi.org/10.1016/j.apm.2015.09.105.
[9] C. Liu, Z.K. Zhang, Information spreading on dynamic social networks, Commun. Nonlinear Sci. 19 (4) (2014) 896–904, http://dx.doi.org/10.1016/j.
[10] Z. Yan, T. Wang, Y. Chen, H. Zhang, Knowledge sharing in online health communities: A social exchange theory perspective, Inf. Manage. 53 (5) (2016) 643–653, http://dx.doi.org/10.1016/j.im.2016.02.001.
[11] W. Liu, S. Zhong, Web malware spread modelling and optimal control strategies, Sci. Rep. 7 (2017) 42308, http://dx.doi.org/10.1038/srep42308.
[12] Y. Zan, J. Wu, P. Li, Q. Yu, SICR rumor spreading model in complex networks: Counterattack and self-resistance, Phys. A 405 (2014) 159–170, http://dx.doi.org/10.1016/j.physa.2014.03.021.
[13] H. Zhu, Y. Kong, J. Wei, J. Ma, Effect of users' opinion evolution on information diffusion in online social networks, Phys. A 492 (2018) 2034–2045, http://dx.doi.org/10.1016/j.physa.2017.11.121.
[14] Y. Liu, S.M. Diao, Y.X. Zhu, Q. Liu, SHIR competitive information diffusion model for online social media, Phys. A 461 (2016) 543–553, http://dx.doi.org/10.1016/j.physa.2016.06.080.
[15] R. Wang, S. Rho, B.W. Chen, W. Cai, Modeling of large-scale social network services based on mechanisms of information diffusion: Sina Weibo as a case study, Future Gener. Comput. Syst. 74 (2017) 291–301, http://dx.doi.org/10.1016/j.future.2016.03.018.
[16] L. Zhao, J. Wang, Y. Chen, Q. Wang, J. Cheng, H. Cui, SIHR rumor spreading model in social networks, Physica A 391 (2012) 2444–2453, http://dx.doi.org/10.1016/j.physa.2011.12.008.
[17] Y. Zan, DSIR double-rumors spreading model in complex networks, Chaos Solitons Fractals 110 (2018) 191–202, http://dx.doi.org/10.1016/j.chaos.2018.03.021.
[18] Z. Chen, Z. Xu, A delayed diffusive influenza model with two-strain and two vaccinations, Appl. Math. Comput. 349 (2019) 439–453, http://dx.doi.org/10.1016/j.amc.2018.12.065.
[19] R.Y. Tian, X.F. Zhang, Y.J. Liu, SSIC model: A multi-layer model for intervention of online rumors spreading, Phys. A 427 (2015) 181–191, http://dx.doi.org/10.1016/j.physa.2015.02.008.
[20] Q. Liu, T. Li, M. Sun, The analysis of an SEIR rumor propagation model on heterogeneous network, Phys. A 469 (2017) 372–380, http://dx.doi.org/10.1016/j.physa.2016.11.067.
[21] C. Wan, T. Li, Z. Sun, Global stability of a SEIR rumor spreading model with demographics on scale-free networks, Adv. Difference Equ. (2017) http://dx.doi.org/10.1186/s13662-017-1315-y.
[22] Z. Yi, C. Chong, A Rumor spreading Model Considering Latent State, in: Proceedings of the Eighth International Conference on Management Science and Engineering Management, Springer Berlin Heidelberg, 2014, http://dx.doi.org/10.1007/978-3-642-55182-6_14.
[23] L. Zhang, C. Su, Y. Jin, M. Goh, Z. Wu, Cross-network dissemination model of public opinion in coupled networks, Inf. Sci. (Ny) 451–452 (2018) 240–252, http://dx.doi.org/10.1016/j.ins.2018.04.037.
[24] Y.A. Kuznetsov, C. Piccardi, Bifurcation analysis of periodic SEIR and SIR epidemic models, J. Math. Biol. 32 (1994) 109–121, http://dx.doi.org/10.1007/bf00163027.
[25] S. Hosseini, M.A. Azgomi, A.T. Rahmani, Malware propagation modeling considering software diversity and immunization, J. Comput. Sci. 13 (2016) 49–67, http://dx.doi.org/10.1016/j.jocs.2016.01.002.

[26] T. Li, Y. Wang, Z. Guan, Spreading dynamics of a SIQRS epidemic model on scale-free networks, Commun. Nonlinear Sci. Numer. Simul. 19 (2014) 686–692, http://dx.doi.org/10.1016/j.cnsns.2013.07.010.
[27] S. Huang, F. Chen, L. Chen, Global dynamics of a network-based SIQRS epidemic model with demographics and vaccination, Commun. Nonlinear Sci. Numer. Simul. 43 (2017) 296–310, http://dx.doi.org/10.1016/j.cnsns.2016.07.014.
[28] S. Hosseini, M. Abdollahi, A model for malware propagation in scale-free networks based on rumor spreading process, Comput. Netw. 108 (2016) 97–107, http://dx.doi.org/10.1016/j.comnet.2016.08.010.
[29] S. Hosseini, M.A. Azgomi, The dynamics of an SEIRS-QV malware propagation model in heterogeneous networks, Phys. A 512 (2018) 803–817, http://dx.doi.org/10.1016/j.physa.2018.08.081.
[30] Y. Zhang, Y. Su, L. Weigang, H. Liu, Rumor and authoritative information propagation model considering super spreading in complex social networks, Phys. A 506 (2018) 395–411, http://dx.doi.org/10.1016/j.physa.2018.04.082.
[31] Y. Liu, B. Wang, B. Wu, S. Shang, Y. Zhang, C. Shi, Characterizing super-spreading in microblog: An epidemic-based information propagation model, Phys. A 463 (2016) 202–218, http://dx.doi.org/10.1016/j.physa.2016.07.022.
[32] F. Xiong, X.M. Wang, J.J. Cheng, Subtle role of latency for information diffusion in online social networks, Chin. Phys. B. 25 (2016) 1–9, http://dx.doi.org/10.1088/1674-1056/25/10/108904.
[33] A. Vespignani, Modelling dynamical processes in complex socio-technical systems, Nat. Phys. 8 (1) (2012) 32–39, http://dx.doi.org/10.1038/nphys2160.
[34] O. Diekmann, J. Heesterbeek, J.A. Metz, On the definition and the computation of the basic reproduction ratio $\mathcal{R}_0$in models for infectious diseases in heterogeneous populations, J. Math. Biol. 28 (1990) 365–382, http://dx.doi.org/10.1007/BF00178324.
[35] W. Yi, J. Cao, Global dynamics of a network epidemic model for waterborne diseases spread, Appl. Math. Comput. 237 (2014) 474–488, http://dx.doi.org/10.1016/j.amc.2014.03.148.
[36] P. Van Den Driessche, J. Watmough, Reproduction numbers and sub-threshold endemic equilibria for compartmental models of disease transmission, Math. Biosci. 180 (2002) 29–48, http://dx.doi.org/10.1016/S0025-5564(02)00108-6.
[37] L. Liu, X. Wei, N. Zhang, Global stability of a network-based SIRS epidemic model with nonmonotone incidence rate, Phys. A 515 (2019) 587–599, http://dx.doi.org/10.1016/j.physa.2018.09.152.
[38] B.K. Sahu, M.M. Gupta, B. Subudhi, Stability analysis of nonlinear systems using dynamic-routh's stability criterion: a new approach, in: Proceedings of the International Conference on Advances in Computing, Communications and Informatics, 2013, pp. 1765–1769, http://dx.doi.org/10.1109/ICACCI.2013.6637448.
[39] A preferential information of Baidu App released by Z.T. Huang on morning of Nov.22, 2018, https://weibo.com/2713968254/H3OKGEnxM?type=repost#_rnd1553607417502.